

WEAK DIFFRACTED SHOCKS NEAR SINGULAR RAYS*

L. TING[†] AND J. B. KELLER[‡]

Abstract. A weak shock incident upon an obstacle produces weak reflected and diffracted shocks. The resulting flow is analyzed near a point P where either the incident shock or a reflected shock meets a diffracted shock. The path of P is called a singular ray, and it is analogous to a ray on a shadow boundary. For self-similar problems, the flow near P is shown to be the solution of a nonlinear elliptic free boundary problem. This flow is regular, in contrast to the singular flow given by linear theory. An analogous problem is found for the interaction of a weak rarefaction wave with a weak shock. Both problems are also applicable to steady self-similar supersonic flows past bodies. Hunter's analysis (SIAM J. Appl. Math. 48, (1988), pp. 1–37.) implies that these problems are canonical, i.e. that they apply to general hyperbolic systems in any number of dimensions. Simplified forms of both problems are solved numerically.

1. Introduction. When a shock wave hits a rigid obstacle, it produces reflected and diffracted shocks, and diffracted expansion waves. They are shown in Figure 1 for the special case of a plane shock incident upon a semi-infinite thin rigid screen. The reflected shock is shown as a straight line segment and the diffracted wave is shown as a circular arc. The figure is based upon linearization of the equations of gas dynamics and the shock conditions about the state of rest. Linearization, expected to be valid for weak waves of strength $\varepsilon \ll 1$, has been used widely in shock wave theory (Lighthill [1], Keller and Blank [2], Ting and Ludloff [3], Ter-Minassiants [4], Ting and Gunzburger [5]) and in supersonic aerodynamics. (see e.g. Ward [6]).

Linearization is not valid at the diffracted wavefront in Figure 1. There it yields a field with a positive infinite outward pressure gradient along AO and BO' , a negative infinite gradient along BO and AO' , and singularities at O and O' . Methods devised by Lighthill [7], [8], Whitham [9], and Hunter and Keller [10], [11] correct linear theory by removing the infinite pressure gradients. They show that negative outward infinite gradients like those along BO and AO' are replaced by weak shocks of strength ε^2 , and that positive outward infinite gradients like those along AO and BO' are replaced by expansion waves with finite positive gradients.

These methods do not apply near O and O' , which according to linear theory, are the points of tangency of the incident and reflected shocks with the diffracted wave. The paths of such points are called singular rays. They correspond to rays along shadow boundaries for time-harmonic waves. The singularities at O and O' can be removed by introducing inner expansions near these points, as was done by Kuo [12], Zahalak and Myers [13], Harabetian [14], Hunter [15], Tabak [16], Bagdoyev [17], and Morawetz [18]. These authors all obtained for the inner solution, a problem of mixed type for the nonlinear transonic small disturbance equation. They obtained it by expanding around the undisturbed state. As a consequence, the nonlinear diffracted shock is partly inside the sonic circle, where the flow is subsonic and the equation is elliptic, and partly outside the sonic circle, where the flow is supersonic and the equation is hyperbolic.

We modify the method of the preceding authors by expanding about the state with the highest characteristic speed near each of the points O and O' . Thus near

*Received December 15, 1999.

[†]Courant Institute of Mathematical Sciences, New York University, 251 Mercer Street, New York, NY 10012, USA.

[‡]Departments of Mathematics and Mechanical Engineering, Stanford University, Stanford, CA 94305-2125, USA (keller@math.stanford.edu). This work supported in part by the AFOSR.

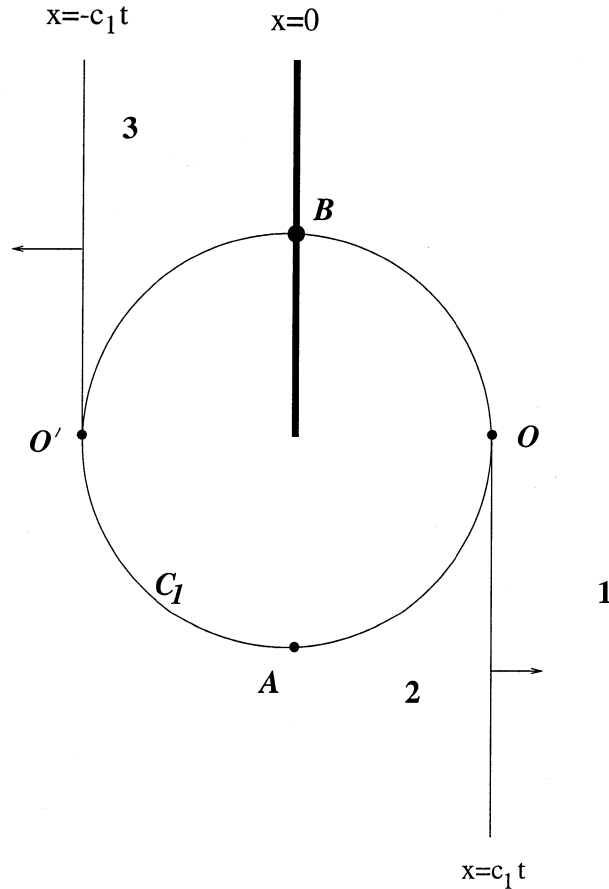


FIG. 1. Configuration at time $t > 0$ after an incident shock traveling to the right hits a thin rigid screen. The screen is shown as a dark line along the positive y -axis. The incident shock and the reflected shock are shown as semi-infinite lines parallel to the y -axis at $x = c_1 t$ and $x = -c_1 t$ respectively. They are tangent to the circle C_1 , of radius $c_1 t$, at O and O' respectively. C_1 bounds the diffracted wave. The pressure is p_1 ahead of the incident shock, p_2 behind it, and p_3 behind the reflected shock. This figure is based upon linearization about the ambient state 1.

O we expand about the state behind the incident shock. See Figure 2. Then the nonlinear diffracted shock is contained entirely within the sonic circle. There the transonic equation for the pressure is purely elliptic. Thus we obtain for the inner solution a nonlinear elliptic free boundary problem instead of a problem of mixed type. Similarly, at O' we expand about the state behind the reflected shock and after normalization we obtain exactly the same problem at O' as at O .

Hunter [15] showed that the problem he obtained for the transonic small disturbance equation is canonical. This means that it applies in the neighborhood of a singular ray for a general class of hyperbolic systems of partial differential equations in any number of dimensions. We shall see that for self-similar problems, his problem in the elliptic region with appropriate conditions on the boundary, is the same as ours. Therefore, our form of the problem is also canonical. In particular, it applies near any point of tangency of a weak shock with a weak diffracted wave, in a self-similar flow.

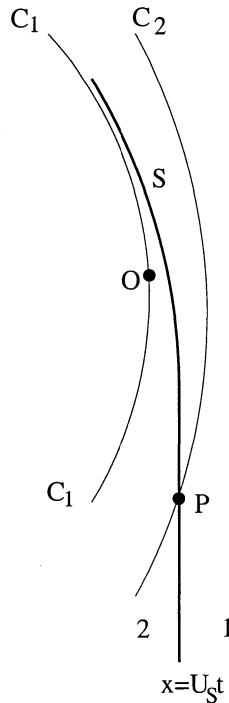


FIG. 2. Exact nonlinear flow configuration near O in Figure 1. The incident shock at $x = U_S t$ has speed $U_S > c_1$. It ends at P where it intersects the circle C_2 of radius $c_2 t$ centered at $(u_2 t, 0)$. The circle C_1 lies inside C_2 . The diffracted shock S starts at P , lies between C_1 and C_2 , and approaches C_1 .

We also formulate a similar problem for the interaction of a weak rarefaction or expansion wave with a weak shock. We can show it to be canonical by Hunter's method [15]. Both canonical problems also apply to steady supersonic flow in three dimensions. An extended abstract of the present work is given in [19].

For simplified forms of the two canonical problems, we construct solutions numerically. These solutions can be used in the first steps of iterative procedures to obtain more accurate solutions.

2. Interaction of a weak incident shock with a weak diffracted shock.

We consider the two dimensional problem of a weak plane shock normal to the x -axis moving in the direction of increasing x . The gas ahead of the shock is at rest in a uniform state denoted 1, and that behind it is in a uniform state denoted 2. At time $t = 0$, the shock hits a thin, rigid screen lying along the positive y -axis. The flow is self-similar for all $t > 0$. Experiment, linear theory, and numerical calculation show that a wave pattern like that shown in Figure 1 results. In addition to the incident shock, there is a reflected shock and a diffracted wave.

Linearization about the state 1, with sound speed c_1 yields the result that the diffracted wavefront at time t is a circle C_1 of radius $c_1 t$ with its center at the tip of the screen. It determines the incident and reflected shocks as semi-infinite lines tangent to C_1 at O and O' respectively. Within this circle, the pressure is $\bar{p} = p_1 + \varepsilon \tilde{p} + O(\varepsilon^2)$. Here p_1 is the pressure in the state of rest ahead of the incident shock and $(p_2 - p_1)/p_1 = 4\gamma\varepsilon(\gamma + 1)^{-1}$ is the strength of the incident shock. The linearized

pressure \bar{p} was determined by Keller and Blank [2] and it was modified by Hunter and Keller [11] to account for nonlinear effects near the diffracted wavefront. The result is that the arcs AO and BO' are replaced by rarefaction waves while the arcs BO and AO' are replaced by shocks. For $x > 0$ the shock near BO and the rarefaction near AO' are slightly outside the circle C_1 .

The exact location at time t of the front of the rarefaction wave near AO is an arc of a circle C_2 of radius $\bar{r}_2 = c_2 t$ with center at $(u_1 t, 0)$, as is shown in Figure 2. This is because it is a characteristic surface of state 2 initiated at the tip of the screen $(0, 0)$ at $t = 0$. The exact location of the incident shock is the semi-infinite straight line $x = U_S t$ with upper endpoint P , where U_S is the shock speed. The arc C_2 intersects the incident shock because a shock is subsonic with respect to the flow behind it. To find the location of the point P of intersection, we express the shock speed U_S and the velocity u_2 behind the shock in terms of ε, c_1 , and the adiabatic exponent γ of the gas:

$$U_S = (c_1 + c_2 + u_2)/2 + O(\varepsilon^2), \quad u_2 = 4\varepsilon(\gamma + 1)^{-1} + O(\varepsilon^2).$$

Then in polar coordinates \bar{r}_2, θ_2 with origin at the center of C_2 , P is given by $\bar{r}_2 = c_2 t, \theta_2 = -\sqrt{2\varepsilon} + O(\varepsilon^{3/2})$. The diffracted shock S starts at P and lies inside the circle C_2 but outside the circle C_1 . Since the flow is continuous across C_2 , both the slope of S and the pressure jump across S must be the same as those of the incident shock at P .

These considerations suggest that to find the flow near P we should expand it about the flow in state 2, which is the state near P with the highest pressure. (Similar considerations applied to O' suggest expanding the flow there about the flow in the state 3 behind the reflected shock.) Therefore we follow the procedure of [13]–[17], introducing an inner expansion near P , but expanding about state 2. Because of self-similarity, the pressure is a function of $r_2 = \bar{r}_2/c_2 t$ and θ_2 . We define the stretched coordinates r, θ by

$$(2.1) \quad r = \frac{1 - r_2}{\varepsilon}, \quad \theta = \frac{\theta_2 + \sqrt{2\varepsilon}}{\sqrt{\varepsilon}}.$$

Then we write the pressure \bar{p} as

$$(2.2) \quad \bar{p} = p_2 [1 + \varepsilon \gamma p(r, \theta)] + O(\varepsilon^2).$$

We find that p satisfies the transonic small disturbance equation

$$(2.3) \quad \{[2r + (\gamma + 1)p]p_r\}_r - p_r + p_{\theta\theta} = 0.$$

To describe the domain in which (2.3) holds, we represent the shock S by $r = f(\theta)$. Then (2.3) holds for $r \geq f(\theta)$ for $\theta \geq 0$, and $r \geq 0$ for $\theta \leq 0$.

The pressure is continuous across C_2 . Therefore the boundary condition along the arc of C_2 below P is

$$(2.4) \quad p = 0 \quad \text{at} \quad r = 0, \quad \theta \leq 0.$$

On the shock S given by $r = f(\theta)$ for $\theta \geq 0$, the following two equations can be derived from the shock conditions and the equations of motion [20]:

$$(2.5) \quad p = -p_1(\theta) - \frac{2[2f + (f')^2]}{\gamma + 1} \quad \text{on} \quad r = f(\theta), \quad \theta \geq 0,$$

$$(2.6) \quad [2f + (f')^2 + (\gamma + 1)p] p_r = -[\theta + 3f'] p'_1(\theta) - 2(1 + f'') \left[p_1(\theta) + \frac{2f + 5(f')^2}{\gamma + 1} \right] \\ \text{on } r = f(\theta), \quad \theta \geq 0.$$

Here $p_1(\theta)$ denotes the pressure ahead of the shock. In the present case, it is a constant:

$$(2.7) \quad p_1(\theta) = -4/(\gamma + 1), \quad \theta \geq 0.$$

Thus $p'_1(\theta) = 0$. In §3, we shall consider a case where $p_1(\theta)$ is not constant.

The shock S is the continuation of the incident shock, so we have at $\theta = 0$,

$$(2.8) \quad f(0) = 0.$$

Finally, as $r \rightarrow \infty$, the pressure must match with the outer solution $\bar{p} = p_1 + \varepsilon \tilde{p} + O(\varepsilon^2)$ given in [2]. By equating (2.2) to this expression, and using the form of \tilde{p} given in [2], we get

$$(2.9) \quad \gamma p(r, \theta) \sim -\frac{4\gamma}{\gamma + 1} \left[\frac{1}{2} + \frac{1}{\pi} \tan^{-1} \frac{\theta}{\sqrt{2r}} \right] \text{ as } r \rightarrow \infty.$$

Here \tan^{-1} lies between $-\pi/2$ and $\pi/2$. The problem for $p(r, \theta)$ and $f(\theta)$ is (2.3)–(2.9).

Now (2.8) shows that at $\theta = 0$ the shock S begins on the unit circle $r_2 = 1$, corresponding to $r = 0$. As $\theta \rightarrow +\infty$, we expect f and p to increase monotonically to constants, and f' to tend to zero. Then (2.5) and (2.6) lead to

$$(2.10) \quad f(\theta) \rightarrow 2, \quad p[f(\theta), \theta] \rightarrow p_1, \quad \text{as } \theta \rightarrow +\infty.$$

When (2.10) holds, the ultimate position of the shock is at $r = 2$, which is inside the sonic circle $r = 0$, as the definition (2.1) of r shows. Then the shock S remains inside the sonic circle C_2 , where (2.3) is elliptic.

Before describing a method for solving this problem, we shall formulate a similar problem for the interaction of a rarefaction or expansion fan with a weak shock. The same method of solution applies to both problems.

3. Interaction of a weak rarefaction wave with a weak shock. Suppose that at $t = 0$ the upper half ($y > 0$) of a rigid plane at $x = 0$ starts to move with velocity $-4\varepsilon(\gamma + 1)^{-1}$ away from a gas in state 2 at rest in the region $x > 0$. Then as Figure 3 shows, this semi-infinite piston produces a planar rarefaction wave parallel to itself moving into the gas, and a diffracted wave. According to linear theory at time t , the diffracted wavefront is a semicircle C_2 of radius $c_2 t$ with its center at the origin. The rarefaction is a discontinuity at $x = c_2 t$, $y > 0$. Behind the rarefaction, but above the diffracted wavefront, the gas is in a uniform state which we call state 1. Inside the semicircle C_2 , linear theory gives for the pressure \bar{p} the self-similar result

$$(3.1) \quad \bar{p} = p_2 - \frac{4\varepsilon\gamma}{\pi(\gamma + 1)} \cos^{-1} \frac{-y}{(c_2^2 t^2 - x^2)^{1/2}}, \quad x^2 + y^2 \leq c_2^2 t^2, \quad x \geq 0.$$

In (3.1), \cos^{-1} is defined to lie between 0 and π . The pressure (3.1) is singular at the point $x = c_2 t$, $y = 0$ where the rarefaction is tangent to the diffracted wave.

Nonlinear theory shows that the rarefaction is of finite width at time $t > 0$, extending from $x = c_2 t$ at its front to $x = (1 - 2\varepsilon)c_2 t$ at its rear, and the gas behind it is in the uniform state 1. See Figure 4. Within the rarefaction the pressure is

$$(3.2) \quad \bar{p}(x, t) = p_2 \left[1 - \frac{2\gamma}{\gamma + 1} (1 - x/c_2 t) \right], \quad 1 - 2\varepsilon \leq \frac{x}{c_2 t} \leq 1.$$

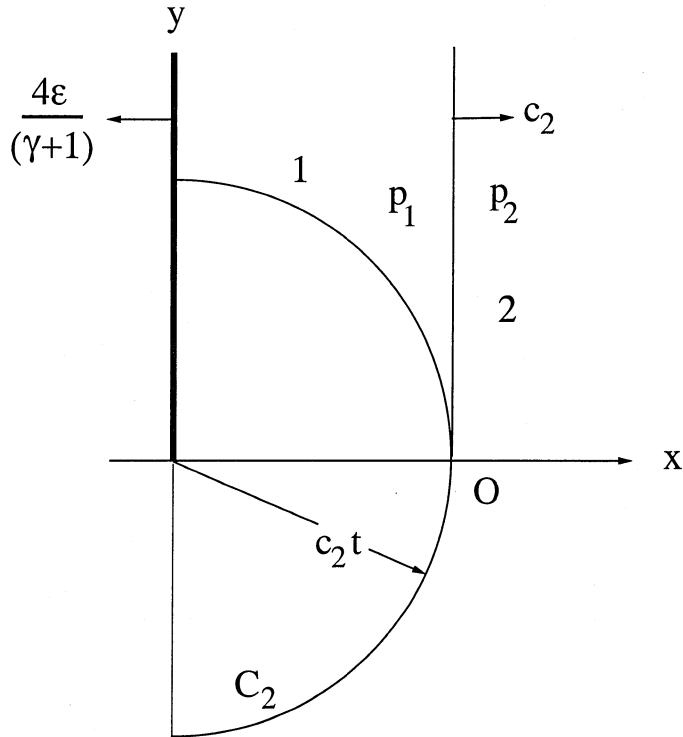


FIG. 3. Configuration at time $t > 0$ after a semi-infinite piston, initially lying along the positive y -axis, is pulled back with speed $-4\epsilon(\gamma + 1)^{-1}$. The gas in $x > 0$ is initially at rest in state 2. Linearization about state 2, on which this figure is based, yields a rarefaction moving to the right with speed c_2 . It is shown as the line $x = c_2t$, $y > 0$. In addition, it yields a diffracted wavefront, shown as the sonic semicircle C_2 of radius c_2t centered at the origin. Behind the rarefaction the gas is in state 1. The rarefaction is tangent to C_2 at the point O .

The methods of [7]–[11] show that the diffracted wavefront in the region $y > 0$ is actually a weak shock S . S starts at the point $x = c_2t$, $y = 0$ on the x -axis where the front of the rarefaction is tangent to the circle C_2 . It extends through the rarefaction into the gas in state 1. There S tends to the circle C_1 of radius c_1t with origin at $x = -4\epsilon t(\gamma + 1)^{-1}$, $y = 0$.

We shall now eliminate the singularity at the point $x = c_2t$, $y = 0$ in the expression (3.1) for the pressure \bar{p} given by linear theory. We proceed exactly as we did in §2 with two differences. First, we define θ differently from the way we did in (2.1) because the shock starts on the x -axis at $\theta_2 = 0$. Therefore we replace (2.1) by

$$(3.3) \quad r = (1 - r_2)/\epsilon, \quad \theta = \theta_2/\sqrt{\epsilon}.$$

Second, although we continue to use (2.7) in state 1 behind the rarefaction fan, we do not use it within the fan. There we use instead (3.2), the value of the pressure in the rarefaction wave, to obtain $p_1(\theta)$. Thus we replace (2.7) by

$$(3.4) \quad \begin{aligned} p_1(\theta) &= -[2f(\theta) + \theta^2]/(\gamma + 1), & 0 \leq f(\theta) + \theta^2/2 \leq 2 \\ p_1(\theta) &= -4/(\gamma + 1), & f(\theta) + \theta^2/2 \geq 2. \end{aligned}$$

Now the problem for the determination of $p(r, \theta)$ and $f(\theta)$ is again (2.3)–(2.9) with (2.7) replaced by (3.4), and the definitions (2.1) replaced by (3.3).

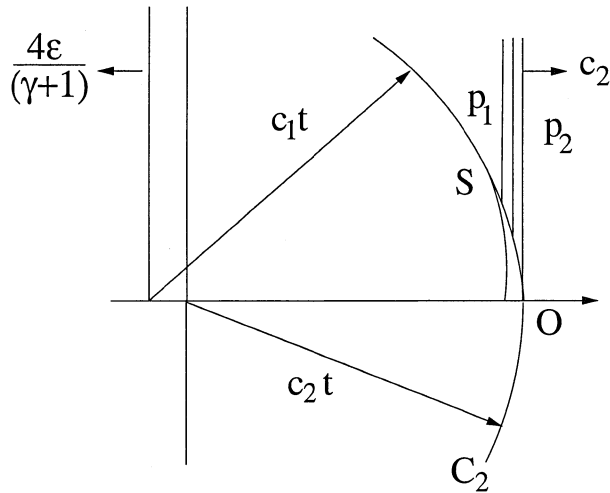


FIG. 4. Flow configuration near the point O in Figure 3, according to nonlinear theory. The rarefaction is of finite width extending from $x = c_2 t$ to $x = (1 - 2\epsilon)c_2 t$. The diffracted wavefront is an arc of the sonic circle C_2 in the region $y < 0$, but it is a shock S in the region $y > 0$. The shock cuts through the rarefaction wave into the gas in state 1. There it approaches the sonic circle C_1 with radius $c_1 t$ and center at $x = -4\epsilon t(\gamma + 1)^{-1}$, $y = 0$.

4. Numerical solution of simplified canonical problems. Now we shall obtain numerical solutions of simplified forms of the two canonical problems. This requires solving (2.3)–(2.9) for $p(r, \theta)$ and $f(\theta)$ for the first problem, and the same equations with (3.4) replacing (2.7) for the second problem. The shock shape $r = f(\theta)$ is defined for $\theta \geq 0$, and the pressure $p(r, \theta)$ is defined for $r \geq f(\theta)$ when $\theta \geq 0$, and $r \geq 0$ when $\theta \leq 0$. We simplify the semilinear equation (2.3) by omitting the nonlinear term $(pp_r)_r$ so that it becomes linear. We also omit pp_r from (2.6). Then we introduce the Busemann variable $\sigma = \sqrt{2}r$, and write the linearized (2.3) for $\hat{p}(\sigma, \theta) = p(\sigma^2/2, \theta)$:

$$(4.1) \quad \hat{p}_{\sigma\sigma} + \hat{p}_{\theta\theta} = 0.$$

This is just Laplace's equation. The domain is $\sigma \geq \sqrt{2f(\theta)}$ for $\theta \geq 0$ and $\sigma \geq 0$ for $\theta \leq 0$.

We begin with a general solution of (4.1) in the half-space $\sigma \geq 0$, which includes the domain above. We write it in terms of a distribution $h(\theta)$ along the θ -axis, and in view of (2.4) we set $h(\theta) = 0$ for $\theta \leq 0$. Thus we write

$$(4.2) \quad \hat{p}(\sigma, \theta) = \frac{1}{\pi} \int_0^{\infty} \frac{h(\theta') \sigma d\theta'}{(\theta - \theta')^2 + \sigma^2}, \quad \sigma \geq 0.$$

We make this solution satisfy the matching condition (2.9) as $r \rightarrow \infty$, and therefore as $\sigma \rightarrow \infty$, by requiring that

$$(4.3) \quad h(\theta) \sim -4/(\gamma + 1) \quad \text{as } \theta \rightarrow +\infty.$$

We shall use (4.2) in the two shock conditions (2.5) and (2.6) to obtain a pair of coupled equations for $f(\theta)$ and $h(\theta)$. Then we shall solve these equations numerically.

For the first problem, we begin by choosing a positive integer N and a positive constant Z_N , and defining $\theta_n = nZ_N/N$, $n = 1, \dots, N$. Then we write $h(\theta)$ in terms

of N constants Y_n :

$$(4.4) \quad h(\theta) = \sum_{n=1}^N Y_n H(\theta - \theta_n) .$$

Here H is the Heaviside function, so $h(\theta) = 0$ for $\theta < \theta_1$ and $h(\theta) = \sum_1^N Y_n$ for $\theta > \theta_N$.

To satisfy (4.3) we require that

$$(4.5) \quad \sum_{n=1}^N Y_n = -4/(\gamma + 1) .$$

When (4.4) is used in (4.2), the integral can be evaluated explicitly with the result

$$(4.6) \quad \hat{p}(\sigma, \theta) = \sum_{n=1}^N Y_n \left[\frac{1}{2} + \frac{1}{\pi} \tan^{-1} \left(\frac{\theta - \theta_n}{\sigma} \right) \right] ,$$

with \tan^{-1} in the range $-\pi/2$ to $\pi/2$.

We now use (4.6) for \hat{p} in the shock condition (2.5), and rewrite the condition in the form

$$(4.7) \quad \begin{aligned} f'(\theta) &= \left\{ 2 - 2f(\theta) - \frac{\gamma + 1}{2} \hat{p} \left(\sqrt{2f(\theta)}, \theta \right) \right\}^{1/2} \\ &= \left\{ 2 - 2f(\theta) - \frac{\gamma + 1}{2} \sum_{n=1}^N Y_n \left[\frac{1}{2} + \frac{1}{\pi} \tan^{-1} \left(\frac{\theta - \theta_n}{\sqrt{2f(\theta)}} \right) \right] \right\}^{1/2} . \end{aligned}$$

When the Y_n are known, this is a first order ordinary differential equation for $f(\theta)$, and (2.8) provides the initial value $f(0) = 0$.

Next we use (4.6) for \hat{p} in the second shock condition (2.6) with pp_r omitted, and recall that $p_r(r, \theta) = \sigma^{-1} \hat{p}(\sigma, \theta)$. We impose (2.6) at the midpoints $\tilde{\theta}_m = (m - \frac{1}{2}) Z_N/N$, $m = 1, \dots, N - 1$ which yields $N - 1$ equations for the N coefficients Y_n in (4.4). These equations are

$$(4.8) \quad \sum_{n=1}^N \frac{\sqrt{2f_m} + (f'_m)^2/\sqrt{2f_m}}{\pi(2f_m + [\tilde{\theta}_m - \theta_n]^2)} [\tilde{\theta}_m - \theta_n] Y_n = \frac{2(1 + f''_m)}{\gamma + 1} [2f_m + 5(f'_m)^2 - 4] ,$$

$$m = 1, \dots, N - 1 .$$

Here $f_m = f(\theta_m)$, etc. The N -th equation is (4.5). When $f(\theta)$ is known, (4.8) and (4.5) are a system of N linear equations for the N coefficients Y_n .

We solve iteratively for $f(\theta)$ and the Y_n , starting with an initial guess for Y_n , say $Y_n^{(0)}$ satisfying (4.5). Then we solve (4.7) and call the solution $f^{(1)}(\theta)$. We use $f^{(1)}(\theta)$ in (4.8) and (4.5) and solve for Y_n , which we call $Y_n^{(1)}$. Then we use $Y_n^{(1)}$ in (4.7) and solve to get $f^{(2)}(\theta)$, etc. With $\gamma = 5/3$, $Z_N = 2.4$ and $N = 3, 4, 6, 8$, the iterates $f^{(j)}(\theta)$ and $Y_n^{(j)}$ converged to a solution in at most 20 iterations. The solution for $f(\theta)$ is shown in Figure 5, and that for the pressure jump across the shock, $p[f(\theta), \theta] - p_1$, is shown in Figure 6.

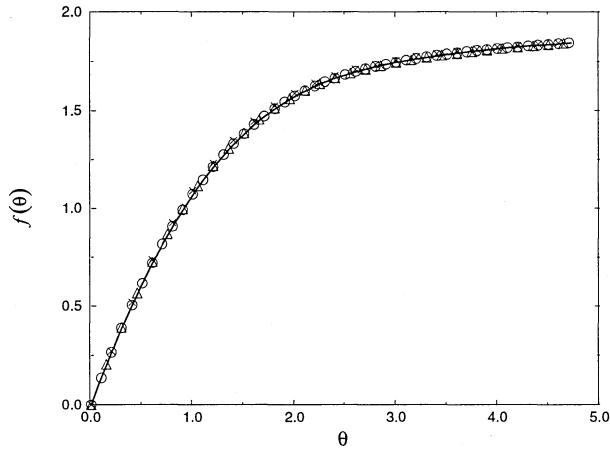


FIG. 5. Graph of $f(\theta)$ as a function of θ for the first canonical problem with $\gamma = 5/3$. The figure is based upon the numerical procedure described in §4. The solid line is drawn through the points for $N = 8$. The \times 's are the results for $N = 3$, Δ 's for $N = 4$, and O 's for $N = 6$. The equation of the shock is $r_2/c_2t = 1 - \varepsilon f \left[\frac{\theta_2}{\sqrt{\varepsilon}} + \sqrt{2} \right]$ where (r_2, θ_2) are polar coordinates with origin at $(u_2t, 0)$ and $\theta_2 = 0$ along the positive x -axis.

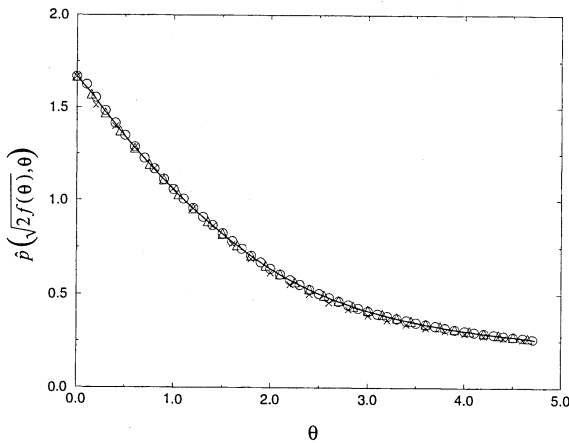


FIG. 6. Graph of $\hat{p} \left(\sqrt{2f(\theta)}, \theta \right)$, the scaled pressure behind the shock, versus θ for the first canonical problem with $\gamma = 5/3$, based on the same calculation as Figure 5. The actual pressure is $\bar{p} = p_2 \left[1 + \varepsilon \gamma \hat{p} \left(\sqrt{2f(\theta)}, \theta \right) \right]$ where $\theta = \frac{\theta_2}{\sqrt{\varepsilon}} + \sqrt{2}$. The symbols have the same meaning as in Figure 5.

To solve the second problem, that involving a rarefaction, we find it advantageous to modify the preceding scheme slightly by adding $p_1(\theta)$, given by (3.4), to the right side of (4.4). Thus we write

$$(4.9) \quad h(\theta) = p_1(\theta) + \sum_{n=1}^N Y_n H(\theta - \theta_n) .$$

Then (4.5) must be replaced by

$$(4.10) \quad \sum_{n=1}^N Y_n = 0 .$$

Finally the use of (4.9) in (4.2) yields, instead of (4.6)

$$(4.11) \quad \hat{p}(\sigma, \theta) = \int_0^\infty \frac{p_1(\theta') \sigma d\theta'}{(\theta - \theta')^2 + \sigma^2} + \sum_{n=1}^N Y_n \left[\frac{1}{2} + \frac{1}{\pi} \tan^{-1} \left(\frac{\theta - \theta_n}{\sigma} \right) \right] .$$

Next we rewrite (2.5) in the form

$$(4.12) \quad f'(\theta) = \left\{ \frac{\theta^2}{2} - f(\theta) - \frac{\gamma+1}{2} \hat{p} \left(\sqrt{2f(\theta)}, \theta \right) \right\}^{1/2}, \quad 0 \leq f(\theta) + \theta^2/2 \leq 2,$$

$$f'(\theta) = \left\{ 2 - 2f(\theta) - \frac{\gamma+1}{2} \hat{p} \left(\sqrt{2f(\theta)}, \theta \right) \right\}^{1/2}, \quad f(\theta) + \theta^2/2 \geq 2 .$$

We use $\hat{p}(\sigma, \theta)$ given by (4.11) in (4.12) to get a first order ordinary differential equation for $f(\theta)$. Similarly, we use (4.11) in (2.6), with the term pp_r omitted, and impose the resulting condition at the $N - 1$ midpoints $\tilde{\theta}_m$. This leads to $N - 1$ equations like (4.8), but with the right side modified due to the use of (3.4) for $p_1(\theta)$ in it. The N -th equation is (4.10).

We solve the equation (4.12) for $f(\theta)$ with $f(0) = 0$, and the modified equations (4.8) and (4.10) for the Y_n . We use the same iteration method as before, starting with $Y_n^{(0)} = 0$. We set $\gamma = 5/3$ and chose $Z_3 = 3.6$, $Z_4 = 4.8$, $Z_5 = 6.0$ and $Z_6 = 7.2$. The results converged in less than 20 iteration. The solution for $f(\theta)$ and $\hat{p} \left[\sqrt{2f(\theta)}, \theta \right]$, which determine the shock shape and the pressure behind the shock, are shown in Figures 7 and 9. Figure 8 shows $\hat{p} \left[\sqrt{2f(\theta)}, \theta \right] - p_1(\theta)$, the pressure jump across the shock. The result for $\hat{p} \left[\sqrt{2f(\theta)}, \theta \right]$ near $\theta = 0$ is not accurate because of the crudeness of the numerical method. Actually $\hat{p} \left[\sqrt{2f(\theta)}, \theta \right]$ should be greater than $p_1(\theta)$.

REFERENCES

- [1] M. J. LIDTHILL, *The Diffraction of blast - I, II*, Proc. Royal Soc., A, 198 (1949), pp. 454-487, 200 (1950), pp. 554-565.
- [2] J. B. KELLER AND A. BLANK, *Diffraction and reflection of pulses by wedges and corners*, Comm. Pure Appl. Math., 4 (1951), pp. 317-328.
- [3] L. TING AND H. F. LUDLOFF, *Aerodynamics of blasts*, J. Aero. Sc., 19 (1952), pp. 317-328.
- [4] S. M. TER-MINASSIANTS, *The diffraction accompanying the regular reflexion of a plane obliquely impinging shock wave from the walls of an obtuse wedge*, J. Fluid Mech., 36 (1969), pp. 391-410.

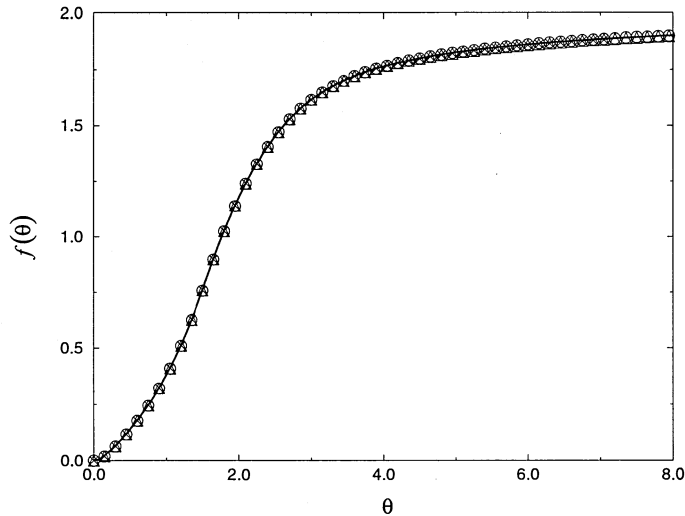


FIG. 7. Graph of $f(\theta)$ versus θ for the second canonical problem with $\gamma = 5/3$, based upon the numerical procedure described in §4. The solid line is drawn through the points for $N = 6$. The \times 's, Δ 's, and O 's are for $N = 3, 4$, and 5 respectively. The equation of the shock is $r_2/c_2t = 1 - \varepsilon f[\theta_2/\sqrt{\varepsilon}]$ where r_2 and θ_2 are defined in the caption of Figure 5.

- [5] L. TING AND M. GUNZBURGER, *Diffraction of Shock Waves by a Moving Thin Wing*, J. Fluid Mech., 42 (1970), pp. 585–608.
- [6] G. N. WARD, *Linearized Theory of Steady High-speed Flow*, Cambridge University Press, Cambridge, 1955.
- [7] M. J. LIDTHILL, *A technique for rendering approximate solutions to physical problems uniformly valid*, Phil. Mag., Series 7, 40 (1949), pp. 1179–1201.
- [8] ———, *The shock strength in supersonic conical flow*, Phil. Mag., Series 7, 40 (1949), pp. 1201–1221.
- [9] G. B. WHITHAM, *Linear and Nonlinear Waves*, John Wiley, New York, 1974.
- [10] J. K. HUNTER AND K. B. KELLER, *Weakly nonlinear high frequency waves*, Comm. Pure Appl. Math., 36 (1983), pp. 547–569.
- [11] ———, *Weak shock diffraction*, Wave Motion, 6 (1984), pp. 79–89.
- [12] Y. H. KUO, J. Aero. Sci., 22 (1954), pp. 504–505.
- [13] G. I. ZAHALAK AND M. K. MEYERS, *Conical flow near singular rays*, J. Fluid Mech., 63 (1974), pp. 537–561.
- [14] E. HARABETIAN, *Diffraction of a weak shock by a wedge*, Comm. Pure Appl. Math., 40 (1987), pp. 849–863.
- [15] J. K. HUNTER, *Transverse Diffraction of Nonlinear Waves and Singular Rays*, SIAM J. Appl. Math., 48 (1988), pp. 1–37.
- [16] E. G. TABAK AND R. R. ROSALES, *Focusing of weak shocks and the von Neumann paradox of oblique shock reflection*, Phys. Fluids, 6 (1991), pp. 1874–1892.
- [17] A. G. BAGDOYEV, *Nonlinear Problems of Compressible Flow*, Israel Prog. for Scientific Translations, Jerusalem, 1969.
- [18] C. S. MORAWETZ, *Potential theory for regular and Mach reflection of a shock at a wedge*, Comm. Pure Appl. Math., 47 (1994), pp. 593–624.
- [19] L. TING AND J. B. KELLER, *Weak shock diffraction and singular rays* (Extended Abstract), ZAMM, 78, Suppl. 2 (1988), S767–770.
- [20] R. COURANT AND K. O. FRIEDRICHS, *Supersonic Flow and Shock Waves*, Interscience, New York, 1948.

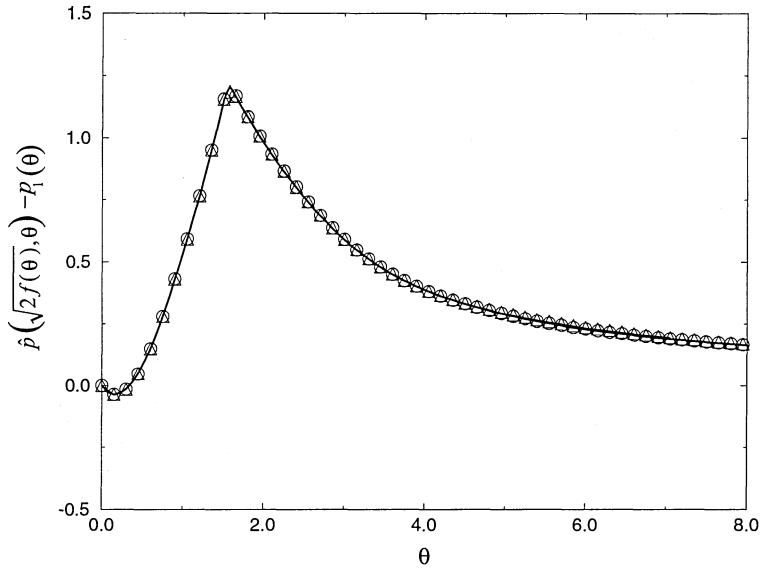


FIG. 8. The jump $\hat{p}(\sqrt{2f(\theta)}, \theta) - p_1(\theta)$ of the scaled pressure across the shock versus θ . The curve is the difference between the two curves in Figure 9, and the symbols have the same meaning as in Figure 7. The actual pressure jump is $\varepsilon\gamma p_2 [\hat{p}(\sqrt{2f(\theta)}, \theta) - p_1(\theta)]$.

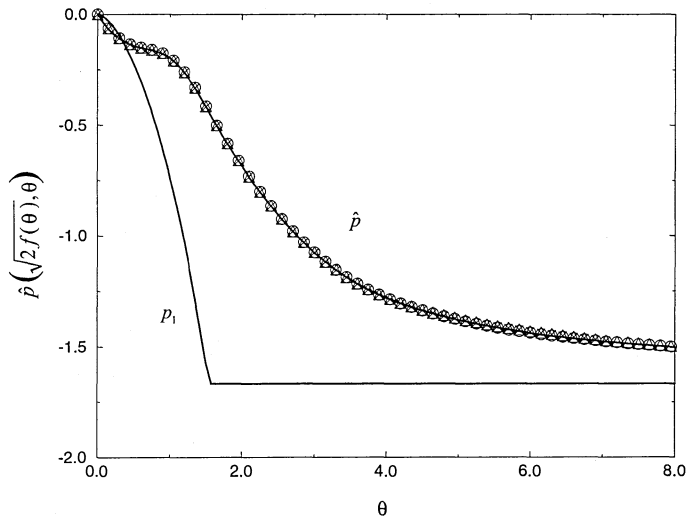


FIG. 9. The upper curve shows $\hat{p}(\sqrt{2f(\theta)}, \theta)$ versus θ for the second canonical problem, where \hat{p} is the scaled pressure behind the shock. The graph is based upon the same calculations as Figure 7, and the symbols have the same meaning. The actual pressure is $\hat{p} = p_2 [1 + \varepsilon\gamma \hat{p}(\sqrt{2f(\theta)}, \theta)]$ where $\theta = \theta_2/\sqrt{\varepsilon}$. The lower curve is $p_1(\theta)$, the scaled pressure ahead of the shock, given by (3.4). The actual pressure is $\bar{p} = p_2 [1 + \varepsilon\gamma p_1(\theta)]$.